Letter

High-speed free-space optical communication using standard fiber communication components without optical amplification

Hua-Ying Liu,[a,*,†] Yao Zhang,[a,†] Xiaoyi Liu,[a] Luyi Sun,[a] Pengfei Fan,[a] Xiaohui Tian,[a] Dong Pan[b], Mo Yuan,[c] Zhijun Yin,[c] Guilu Long,[b] Shi-Ning Zhu,[a] and Zhenda Xie[a,*]

[a]Nanjing University, College of Engineering and Applied Sciences, and Collaborative Innovation Center of Advanced Microstructures, School of Electronic Science and Engineering, School of Physics, National Laboratory of Solid State Microstructures, Nanjing, China
[b]Beijing Academy of Quantum Information Sciences, Beijing, China
[c]Xin Lian Technology Co., Ltd., Huzhou, China

Abstract. Free-space optical communication (FSO) can achieve fast, secure, and license-free communication without physical cables, providing a cost-effective, energy-efficient, and flexible solution when fiber connection is unavailable. To achieve FSO on demand, portable FSO devices are essential for flexible and fast deployment, where the key is achieving compact structure and plug-and-play operation. Here, we develop a miniaturized FSO system and realize 9.16 Gbps FSO in a 1 km link, using commercial single-mode-fiber-coupled optical transceiver modules without optical amplification. Fully automatic four-stage acquisition, pointing, and tracking systems are developed, which control the tracking error within 3 μrad, resulting in an average link loss of 13.7 dB. It is the key for removing optical amplification; hence FSO is achieved with direct use of commercial transceiver modules in a bidirectional way. Each FSO device is within an overall size of 45 cm $\times$ 40 cm $\times$ 35 cm, and 9.5 kg weight, with power consumption of ~10 W. The optical link up to 4 km is tested with average loss of 18 dB, limited by the foggy test environment. With better weather conditions and optical amplification, longer FSO can be expected. Such a portable and automatic FSO system will produce massive applications of field-deployable high-speed wireless communication in the future.

Keywords: free-space optical communication; acquisition, pointing, and tracking system; field-deployable system.

Free-space optical communication (FSO) has received increasing attention as an alternate to fiber communication for high-bandwidth wireless data transmission,[1–4] and it can be built in different scales for various applications. In a space-wide scale, FSO is the key to establishing high-speed satellite internet like Starlink for global network coverage.[5–9] In the near-ground low-altitude scale, FSO is also attractive for its capability of providing high-data-rate, license-free and high-security connection in a relatively small region for applications, including last-mile connection, disaster recovery, and military communication.[10–16]

In these flexible communication scenarios, a portable and plug-and-play FSO system is essential. To establish FSO links, flexible, fast, and fully automatic acquisition, pointing, and tracking (APT) systems are necessary, which requires a complex sensing system and processing algorithm for fast pointing status detection and automatic tracking loop feedback. On the other hand, the portability is also important for flexible field deployment on demand, which requires the FSO system to be miniaturized, integrated, and lightweight for easy handling. However, it can be challenging to pack APT systems in small sizes while keeping high tracking accuracy for sufficiently low link loss, especially over some distance. One common method is to use optical amplifiers like erbium-doped optical fiber amplifiers (EDFAs)[17–20] to compensate for the high link loss, but that inevitably increases

*Address all correspondence to Hua-Ying Liu, liuhuaying@nju.edu.cn; Zhenda Xie, xiezhenda@nju.edu.cn

†These authors contributed equally to this work.

Table 1 Sample of performance of recent FSO systems.

Link type	Working distance	Transmission data rate	Optical amplification	Optical aperture	Weight	Size	Optical amplification	Power consumption	Tracking error	Link loss	Reference
Satellite-ground	400,000 km	622 Mbps (downlink)	Yes	100 mm (satellite) 4× 400 mm (ground)	30 kg	—	Yes	~90 W	10 μrad	—	Ref. 13
Airborne-ground	50 km	1.25 Gbps	Yes	600 mm (ground)	—	—	Yes	—	20 μrad	45 dB (20 km) 56 dB (40 km)	Ref. 14
Airship-ship	20 km	1.5 Gbps	Yes	120 mm	—	—	Yes	—	5 μrad	—	Ref. 8
Helicopter-helicopter	17.5 km	1.5 Gbps	Yes	120 mm	—	—	Yes	—	6.2 μrad	—	Ref. 9
Fixed-wing aircraft-fixed-wing aircraft	136 to 144 km	2.5 Gbps	Yes	120 mm	—	—	Yes	—	5.5 μrad	58.3 dB	
Satellite-ground	450 km	50/100 Mbps	Yes	400 mm (ground)	2.3 kg (satellite)	10 cm × 10 cm × 17 cm (satellite)	Yes	22 W (satellite)	421 μrad	—	Ref. 15
UAV-ground	7 km	—	—	50 mm (UAV)	~8 kg	—	—	—	358 μrad (azimuth) 617 μrad (pitch)	—	Ref. 16
Fixed end-RCEV	1 km	9.16 Gbps	No	90 mm	9.5 kg	$45 \times 40 \times 35$ cm^3	No	10 W	3 μrad	13.7 dB	Our work

system complexity, power consumption, and weight to some extent, as some of the samples shown in Table 1.

Here we demonstrate FSO at 1 km distance with a data rate of 9.16 Gbps using a pair of commercial fiber-optical communication transceiver modules without optical amplification. Low average link loss of 13.7 dB, for the coupling into a single-mode fiber (SMF), is measured using our FSO devices, which is key for this demonstration of bidirectional optical communication. Such low link loss is enabled by the low-diffraction optical design, fully automatic four-stage closed-loop feedback control, and the motion stabilization system in our APT units. Without the need for optical amplifiers, a single FSO device only weighs 9.5 kg, within a size of 45 cm × 40 cm × 35 cm and power consumption of ~10 W. Through integration of multisensors and the development of a corresponding algorithm, automatic, fast, and accurate acquisition and fine-tracking can be achieved within 10 min. Such an FSO device can be used in a pair for a single link or more pairs for multiple links in a plug-and-play manner to establish FSO channels in minutes, and thus fulfills the demand of field-deployable high-speed data transmission.

The scheme of our FSO communication is shown in Fig. 1(a), and a pair of FSO devices are used at two nodes with separation between 1 and 4 km. Alice is fixed at the top floor in our building, and Bob is loaded on a radio-controlled electric vehicle (RCEV) so that it can move around to change the
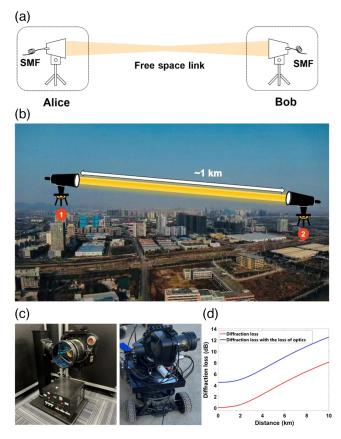
FSO link distance for the experiments, as shown in Fig. 1(b). At both ends, our FSO devices feature identical optical aperture and mechanical design, as shown in Fig. 1(c). Each FSO device consists of an optical transceiver module, an APT unit and its control electronics, and both the transceiver module and the control electronics are sealed in a box for outdoor operation. Both FSO nodes are SMF-coupled, so that bidirectional optical communication can be achieved by the direct use of commercial optical transceiver modules. We choose the optical aperture of 90 mm in diameter and study the diffraction loss of the FSO link as a function of link distance. The result is shown in Fig. 1(d) and <12.7 dB low diffraction can be calculated within a link distance of 10 km, considering the internal transmission of our optics.

Figure 2(a) shows the design of an FSO device. The blue part on the left shows the schematic of the optical part in an APT system, which is mounted on the three-axis gimbal stage for coarse tracking and active stabilization. The optical antenna is in a reflective Cassegrain design with 90 mm optical diameter and scale factor of 10:1, which is followed by the fine tracking optics. Three beacon laser (BL) diodes are used for the three-stage optical tracking, where BL0 (940 nm) and BL1 (638 nm for Alice, 660 nm for Bob)/BL2 (808 nm for Alice, 852 nm for Bob) are for the coarse tracking and first/second-stage fine tracking, respectively. Three complementary metal oxide semiconductor sensors (CMOS), CMOS0 and CMOS1/CMOS2, are used to generate the error signals for coarse tracking and first/second-stage fine tracking, respectively. The divergent angles of the three BLs are designed to be overlapped with each other so that APT process can be achieved stage by stage. While the beacon beam from BL0 and CMOS0 are placed off-axis from the signal beam, the beacon beam from BL1 and BL2 are concentric to the signal beam. The beacon beam from BL2 is from the same fiber as the FSO signal, and a wavelength division multiplexer (WDM) filter is used to separate this BL and communication signal. This fiber is connected to the optical transceiver module, with an optical circulator in between, for the separation of the up/down link optical signals.

With Bob moving on the RCEV, the FSO link can be established within 10 min using our APT systems once settled. The operation schematic of the APT system is shown in Fig. 2(b); its left part shows the mechanism of the active stabilization, initial acquisition, and coarse tracking processes using a three-axis gimbal in the APT system. The active stabilization is achieved using the rotational angular acceleration signal from an inertial measurement unit (IMU). This active stabilization isolates the APT system from the mechanical vibration during the FSO and ensures link stability. In the initial acquisition loop, the IMU is used to record the geomagnetic direction, the acceleration and angular acceleration, and a real-time kinematic (RTK) module is used to record the absolute position of the FSO device. By sharing these parameters between Alice and Bob, the relative angles between the two FSO devices, and thus pointing angles for both FSO devices, can be calculated by the designed algorithm. Then the initial acquisition is performed by feeding the pointing angles between Alice and Bob to the three-axis gimbal. After that, CMOS0 can detect the coarse tracking beam from BL0 in the opposite communication node for the error signal generation and takes over the control of the three-axis gimbal. Then the APT systems are ready for the fine optical tracking. CMOS1 detects the fine-tracking beam from BL1 and feeds back the error signal into FSM1, and a second-stage fine tracking is
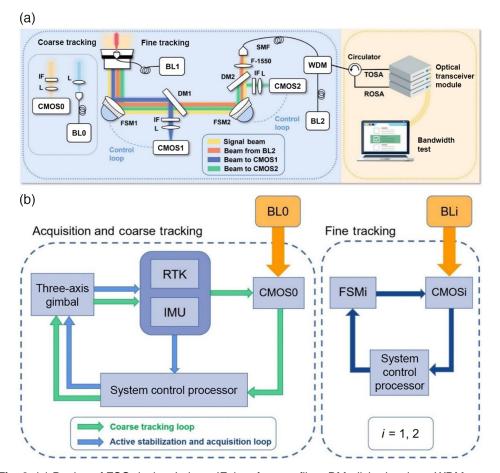

(a)

(b)

(c)   (d)

Fig. 1 (a) Scheme of our FSO. (b) Picture of the 1 km experimental field. (c) Picture of the FSO devices. Alice is fixed in the building and Bob is loaded on an RCEV. (d) Diffraction loss of our FSO system. Red, diffraction loss only; blue, diffraction loss with loss of optics.

(a)

(b)

Fig. 2 (a) Design of FSO device. L, lens; IF, interference filter; DM, dichroic mirror; WDM, wavelength division multiplexer; TOSA, transmitter optical subassembly module; ROSA, receiver optical subassembly module; CMOS, complementary metal oxide semiconductor; BL, beacon laser; and FSM, fast steering mirror system ($i = 1, 2$). (b) Operation schematic of the APT system for acquisition, coarse tracking (left), and fine tracking (right).

performed using CMOS2 and FSM2 in a similar mechanism to further increase the tracking accuracy on top of the first-stage fine-tracking loop, as shown in the right part of Fig. 2(b). The detailed parameters of the APT system are shown in Table 2.

We first measure the performance of the APT system in a 1 km FSO link. Figure 3(a) shows a tracking error with only coarse tracking open in a 120 s measurement, and the average error is 24 μrad, with standard deviation of 34.6 and 20.9 μrad for pitch and azimuth direction, respectively. Then we conduct a measurement of fine-tracking performance, with the result shown in Fig. 3(b). Only coarse tracking is open in the first 30 s, and the fine-tracking control is activated in the following 60 s. The result shows that once the first- and second-stage fine tracking is tuned on, the average tracking error is reduced rapidly from 24 to 3 μrad, with standard deviation of 2.9 and 3.9 μrad for pitch and azimuth direction, respectively. We measure the optical transmission loss using this FSO link, with results shown in Fig. 4(a). An average link loss is measured to be 29.3 dB with only first-stage fine tracking turned on (blue curve). The red curve shows the link loss with the second-stage fine tracking turned on and it reaches 13.7 dB, with standard deviation of 1.4 dB.

Then we use a pair of standard commercial fiber-optical transceiver modules for the FSO measurement. Both modules are rated at 10 Gbps, where the transmitter optical subassembly (TOSA) and receiver optical subassembly (ROSA) modules are both SMF-coupled in each module, as shown in Fig. 4(b). We first test the performance of these modules by direct fiber connections between Alice and Bob in their TOSA and ROSA ports, respectively. Using adjustable optical attenuators, identical losses can be applied for both links. The data rate is measured following the transmission control protocol via the software "open-source tool iperf3" (ESnet and Lawrence Berkeley National Laboratory).[21] As shown in Fig. 4(c), the average data rate is measured at 9.27 Gbps during a 100 s test, and a maximum link loss exceeds 24.1 dB to reach such full bandwidth operation using these modules. Through the 1 km FSO link, the average data rate is measured to be 9.16 Gbps in a 100 s test, with a standard deviation of 0.24 Gbps. Hence, an almost identical data rate is achieved in the FSO link.

We further measure the APT performance in a 4 km FSO link, where the average link loss is measured to be 18 dB with standard deviation of 2.8 dB, as shown in Fig. 5. Compared with the 1 km link, the average link loss increases 4.3 dB.

Table 2 Performance of the APT system.

Component		Value
Coarse-tracking mechanism	Type	Three-axis motorized Gimbal stage
	Tracking range	Azimuth: ± 90 deg
		Pitch: ± 60 deg
		(With roll fixed)
Coarse-tracking sensor	Type	CMOS
	FOV	0.04 rad * 0.04 rad
	Size and frame rate	288 * 288 pixels and 1 kHz
BL0	Power	1 W
	Wavelength	940 nm
	Divergence	35 mrad
Fine-tracking mechanism	Type	FSM
	Range	± 212 μrad
Fine-tracking sensor	Type	CMOS
	FOV	13 mrad * 10 mrad
	Size and frame rate	288 * 288 pixels and 1 kHz
BL1	Power	5 mW
	Wavelength	638 nm and 660 nm
	Divergence	6 mrad
BL2	Power	5 mW
	Wavelength	808 nm and 852 nm
	Divergence	6 mrad

Fig. 3 Performance of the APT system measured with 1 km separation. (a) Coarse tracking error. (b) Fine tracking error.

The maximum loss is 27.8 dB, which exceeds the tolerable maximum loss of the transceiver module. Hence, stable FSO link can hardly be achieved. Our experiment was conducted during the foggy winter in Nanjing with the air visibility generally around 4 to 5 km, which corresponds to absorption loss of ~4 dB at a 4 km distance.[22] With better air quality or more sensitive optical transceiver module, we believe our FSO system can achieve optical communication at 4 km or longer distances.

In this work, we demonstrate 1 km FSO with a data rate of 9.16 Gbps using a pair of commercial fiber optical transceiver modules without optical amplification. This result shows that an FSO network may be achieved using standard fiber communication devices and network technology. Compact FSO devices are developed, with weight of only 9.5 kg. It is fast-field deployable and can be installed on an RECV for quick link change and FSO established within 10 min. We test our FSO link up to 4 km, and a maximum loss of 27.8 dB is measured. At such a loss level, FSO with the same high data rate can be expected at a longer range to a few kilometers with the use of EDFAs. In this experiment, we only test the FSO with both nodes fixed. Actually, our FSO system can also work when the RCEV is moving slowly and hence a mobile FSO link might be expected in a following study. Besides the classical FSO application, our compact APT systems can also be used to establish low-loss quantum links for transmission of quantum information.[23,24]

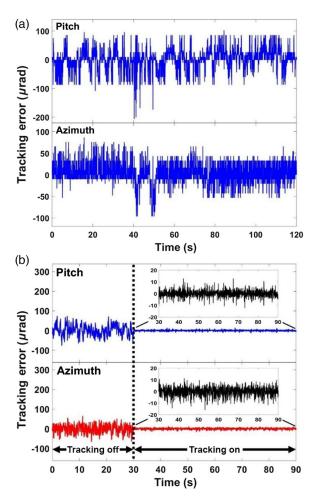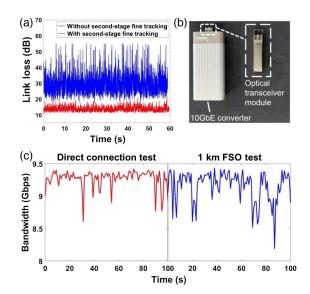

Fig. 4 (a) Link loss for 1 km FSO. (b) Picture of the optical transceiver modules. (c) Communication bandwidth measurement for the module test and FSO. Red, direct connection test; blue, 1 km FSO test.
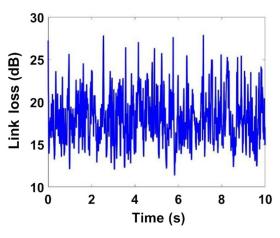
Fig. 5 Link loss for 4 km FSO.

Code, Data, and Materials Availability

The data that support the findings of this study are available from the corresponding author on reasonable request.

References

1. W.-S. Tsai et al., "A 20-m/40-Gb/s 1550-nm DFB LD-based FSO link," *IEEE Photonics J.* **7**(6), 1–7 (2015).
2. H. Henniger and O. Wilfert, "An introduction to free-space optical communications," *Radioengineering* **19**(2), 203–213 (2010).
3. M. A. Khalighi and M. Uysal, "Survey on free space optical communication: a communication theory perspective," *IEEE Commun. Surv. Tut.* **16**(4), 2231–2258 (2014).
4. H. Kaushal et al., "Free-space optical channel models," in *Free Space Optical Communication*, B. Mukherjee, Ed., pp. 41–89, Springer (2017).
5. M. Toyoshima, "Recent trends in space laser communications for small satellites and constellations," *J. Lightwave Technol.* **39**(3), 693–699 (2020).
6. A. B. Raj and A. K. Majumder, "Historical perspective of free space optical communications: from the early dates to today's developments," *IET Commun.* **13**(16), 2405–2419 (2019).
7. H. Kaushal and G. Kaddoum, "Optical communication in space: challenges and mitigation techniques," *IEEE Commun. Surv. Tut.* **19**(1), 57–96 (2016).
8. X.-M. Li, Z.-Z. Li, and X.-M. Li, "Airborne space laser communication system and experiments," *Proc. SPIE* **9795**, 97950G (2015).
9. X.-M. Li et al., "Airborne laser communication technology and flight test," *Proc. SPIE* **9795**, 97950E (2015).
10. A. Jahid, M. H. Alsharif, and T. J. Hall, "A contemporary survey on free space optical communication: potentials, technical challenges, recent advances and research direction," *J. Netw. Comput. Appl.* **200**, 103311 (2022).
11. E. Farooq, A. Sahu, and S. K. Gupta, "Survey on FSO communication system—limitations and enhancement techniques," in *Optical and Wireless Technologies: Proceedings of OWT 2017*, Springer, Singapore, pp. 255–264 (2018).
12. M. Tornatore et al., "A survey on network resiliency methodologies against weather-based disruptions," in *8th Int. Workshop on Resilient Netw. Des. and Model. (RNDM)*, IEEE (2016).
13. B. S. Robinson et al., "The NASA lunar laser communication demonstration—successful high-rate laser communications to and from the moon," in *SpaceOps 2014 Conf.*, p. 1685 (2014).
14. F. Moll et al., "Demonstration of high-rate laser communications from a fast airborne platform," *IEEE J. Sel. Areas Commun.* **33**(9), 1985–1995 (2015).
15. T. S. Rose et al., "Optical communications downlink from a 1.5 U CubeSat: OCSD program," *Proc. SPIE* **11180**, 111800J (2019).
16. C.-X. Tu et al., "A lower size, weight acquisition and tracking system for airborne quantum communication," *IEEE Photonics J.* **14**(6), 1–8 (2022).
17. M. Karimi and M. Nasiri-Kenari, "Free space optical communications via optical amplify-and-forward relaying," *J. Lightwave Technol.* **29**(2), 242–248 (2011).
18. S. Kumar, "Enhancing performance of coherent optical OFDM FSO communication link using cascaded EDFA," *Wireless Personal Commun.* **120**, 1109–1123 (2021).
19. S. H. Alnajjar, A. A. Noori, and A. A. Moosa, "Enhancement of FSO communications links under complex environment," *Photonic Sens.* **7**(2), 113–122 (2017).
20. M. Singh, "Mitigating the effects of fog attenuation in FSO communication link using multiple transceivers and EDFA," *J. Opt. Commun.* **38**(2), 169–174 (2017).
21. ESnet and Lawrence Berkeley National Laboratory, "open-source tool iperf3," GitHub https://github.com/esnet/iperf.
22. L. Jingzhen, *Handbook of Optics*, Xi'an Science and Technology Press, Xi'an (2010).
23. D. Pan et al., "Experimental free-space quantum secure direct communication and its security analysis," *Photonics Res.* **8**(9), 1522–1531 (2020).
24. D. Pan, X.-T. Song, and G.-L. Long, "Free-space quantum secure direct communication: basics, progress, and outlook," *Adv. Devices Instrum.* **4**, 0004 (2023).